

HOSTED BY

Contents lists available at ScienceDirect

Engineering Science and Technology, an International Journal

journal homepage: www.elsevier.com/locate/jestech

Full Length Article

Importance of thermal radiation from heat sink in cooling of three phase PWM inverter kept inside an evacuated chamber

Anjan Sarkar*, Basil Issac

AMETEK Instruments India Private Limited, Bangalore, India

ARTICLE INFO

Article history:

Received 14 April 2016

Revised 23 May 2016

Accepted 7 June 2016

Available online xxx

Keywords:

IGBT

Thermal radiation

Heat sink

SPWM technique

Junction temperature

ABSTRACT

The paper describes a thermal analysis of a three-phase inverter operated under a Sinusoidal Pulse Width Modulation (SPWM) technique which used three sine waves displaced in 120° phase difference as reference signals. The IGBT unit is assumed to be placed with a heat sink inside an evacuated chamber and the entire heat has to be transferred by conduction and radiation. The main heat sources present here are the set of IGBTs and diodes which generates heat on a pulse basing on their switching frequencies. Melcosim (a well-known tool developed by Mitsubishi Electric Corporation) has been used to generate the power pulse from one set of IGBT and diode connected to a phase. A Scilab code is written to study the conduction and thermal radiation of heat sink and their combined effect on transient growth of the junction temperature of IGBT unit against complex switching pulses. The results mainly show that how thermal radiation from heat sink plays a crucial role in maintaining the junction temperature of IGBT within a threshold limit by adjusting various heat sink parameters. As the IGBT heat generation rate becomes higher, radiative heat transfer of the heat sink increases sharply which enhances overall cooling performance of the system.

© 2016 The Authors. Production and hosting by Elsevier B.V. on behalf of Karabuk University. This is an open access article under the CC BY-NC-ND license (<http://creativecommons.org/licenses/by-nc-nd/4.0/>).

1. Introduction

In recent years, effort to spread the use of renewable energy sources with depleting layers of hydrocarbon fuels has been increased. To utilize these renewable energy resources, an inverter is essential which converts DC to AC as most of the renewable energy is found in DC form. The inverter mainly consists of IGBT (i.e. voltage controlled power transistor) that is used while voltage requirement increases. IGBT (Insulated Gate Bipolar Transistor) improves dynamic performance, efficiency and dissipates heat in the form of conduction as well as switching losses. A heat sink attached to IGBT cold plate drives the heat away from the module to external ambient. Kojima et al. [1] describes a novel electro-thermal coupling simulation technique for analysing automotive IGBT modules. The transient temperature response obtained using the proposed model was validated with FEM model and the experimental results. In their approach, they could successfully capture the lateral thermal spreading and thermal interferences occurring at IGBT module. Popovic et al. [2] conducted a thermal analysis of the half bridge IGBT power module mounted on a heat sink.

They approached with FEM and verified that temperature rise of the system for different cases of power dissipation and forced cooling condition. Finally, they found good agreement between their model and the experiments. Ke Ma et al. [3] highlighted the discrepancies of Foster type of RC network in addressing the thermal impedances of heat sink and thermal grease. They proposed a new thermal model which gave a better result for both junction and case temperature compared to the earlier model. Schnell [4] numerically calculated switching and conduction losses under the assumption of sinusoidal output currents. Static and transient temperature rise in the module with specific heat sink is calculated inside the program. Losses in the IGBT and companion freewheeling diode are iteratively adjusted to temperature rises. Angira et al. [5] used a float metal concept to reduce RF overlap area between the movable structure of capacitive shunt RF-MEMS switch and central conductor of CPW for improving the insertion loss of the device without affecting the down state response. Pal et al. [6] has performed an analytical study of dual material surrounding Gate MOSFET (DMSG) by solving Poisson equation. In their results they have revealed that DMSG MOSFET provides higher efficacy to prevent short channel effects as compared to conventional MOSFET. Moaiyeri et al. [7] have simulated 32 nm CNTFET model and demonstrated improvements in terms of speed and power delay product as compared to the cutting edge CNTFET based

* Corresponding author.

E-mail addresses: anjan.sarkar@ametek.com, anjansarkar@gmail.com (A. Sarkar), basil.issac@ametek.com, basilisaac@yahoo.com (B. Issac).

Peer review under responsibility of Karabuk University.

Nomenclature

A	exposed surface area to ambient (m^2)
B	ratio of fin thickness (t) to base thickness (t_b)
C_p	specific heat of copper (J/kg K)
F	view factor
f	frequency (Hz)
h	heat transfer coefficient ($\text{W/m}^2 \text{K}$)
H	height of the heat sink fin (m)
I	applied current (A)
k	thermal conductivity of copper (W/m K)
l	equivalent height of heat sink along the heat transfer direction ($H/2$) (m)
L	length of the heat sink fin (m)
M	modulation factor
n	number of fins of the heat sink
PF	power factor ($\cos \phi$)
P	power (W)
Q	heat transferred (W)
R	thermal resistance (K/W)
R'	electrical resistance (Ω)
S	gap between fins of the heat sink (m)
t	thickness (m)
t'	time (s)
ts'	time to reach steady state condition (s)
T	absolute temperature (K)
V	operating voltage (V)
W	width of heat sink base (m)

Greek alphabets

ρ	density of copper (kg/m^3)
η	overall surface efficiency of heat sink fins
ε	emissivity of the heat sink surface
σ	Stefan–Boltzmann constant (5.67×10^{-8}) ($\text{W/m}^2 \text{K}^4$)
ϕ	phase angle (deg)

Subscripts

a	ambient
av	average
b	heat sink base
c	case
C	collector
CD	conduction
CE	collector-emitter
ch	heat sink channel
cs	case to sink
d	dissipation
G	gate
hs	heat sink
O	output
r	radiative
rr	reverse recovery
sa	sink to ambient
sat	saturated
SW	switching

ternary designs. Turkiymazoglu [8] used water nanofluid for performance enhancement of a direct absorption solar collector by increasing the thermal efficiency. He developed analytical solutions of the temperature fields for the two dimensional steady state model to study the increase in temperature of the heat transferring nanofluid. In the above literatures the thermal radiation is considered negligible and hence become an interesting field to be researched for its effect on a IGBT under operating condition and hence the present study is focused to that.

2. Objective of research

In the present investigation, a three phase inverter is subjected to a voltage source that use PWM switching techniques having a DC input voltage of constant magnitude. The inverter job is to take this DC input to generate AC output, where the magnitude and frequency can be controlled. The entire unit has to be placed in an evacuated chamber where force cooling mechanism can't be adapted and hence huge amount of heat generated inside has to be removed to the atmosphere by means of conduction and radiation. Keeping in mind of above condition, the study has been conducted thoroughly to maximize radiation heat transfer of a plate fin heat sink which is further attached to this unit for removal of the total heat produced inside.

3. SPWM technique and input conditions applied

In this design the Sinusoidal Pulse Width Modulation (SPWM) technique has been used for controlling the inverter to produce desired output voltage and frequency. SPWM technique is widely used in power electronics to digitize the power so that a sequence of voltage pulses can be generated by the on and off of the power switches. The inverter assembly consists of three IGBT

(CM150DY-34A/Mitsubishi Electric) modules connected to three different output phases as shown in Fig. 1. Each module consists of two IGBT transistors which are attached to their freewheeling diodes, in turn making a total of six transistors and six diodes inside the whole assembly. The input conditions considered for this investigation are given below for the complete inverter assembly.

$$V = 1000 \text{ V}, PF = 0.7, M = 1, f_{sw} = 3 \text{ kHz}, f_o = 60 \text{ Hz}, R'_G = 3.2 \Omega,$$

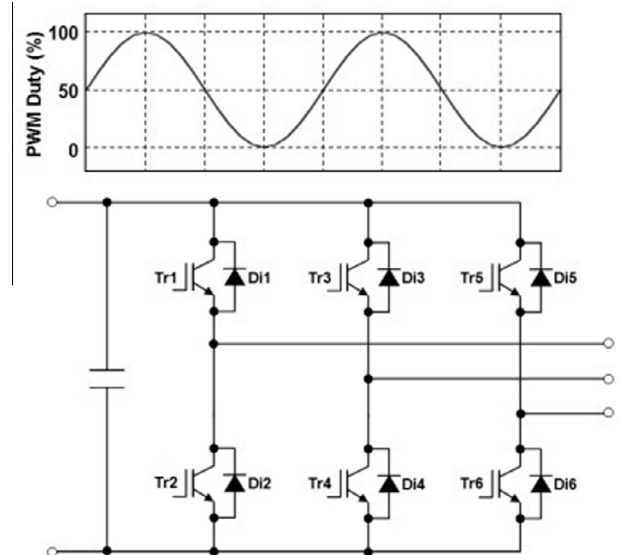


Fig. 1. IGBT transistors and freewheeling diode architecture inside three phase inverter.

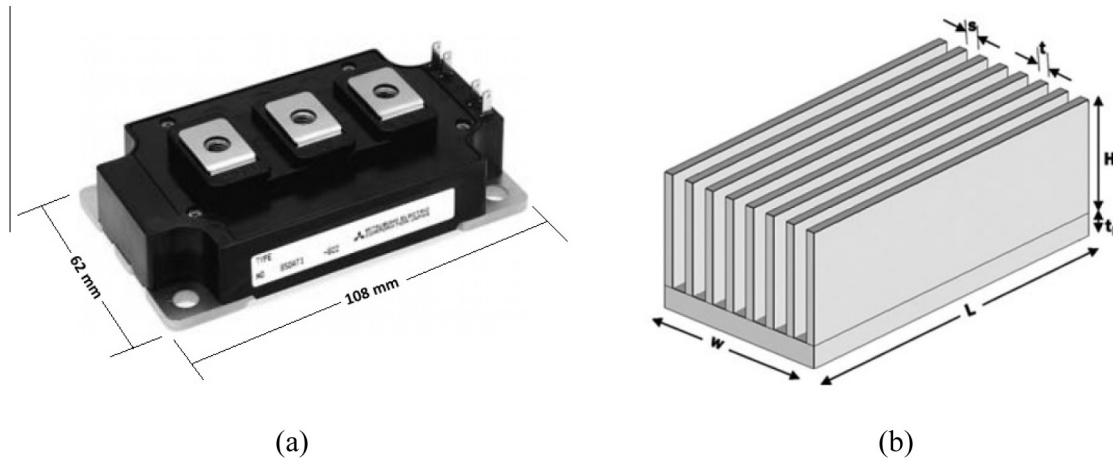


Fig. 2. Schematic of an IGBT module and a plate finned heat sink.

For easiness of calculation the value of R_{jc} is considered as 0.1 for both diode and transistor throughout the entire study. For better understanding of the reader, a basic schematic of an IGBT module and the heat sink has been shown in Fig. 2 below.

3.1. IGBT modelling

With the above input conditions, MELCOSIM (Software by Mitsubishi Electric Corporation) software is used to calculate the

heat generated by IGBT transistors and diodes. Output current and voltage waveform for one of the phase is shown in Fig. 3a, where voltage seems to lead the current because of an inductive load on the circuit. To avoid clumsiness, waveform of other two phases are not shown inside the above figure. With the above inputs transient power dissipation by the complete inverter unit is calculated for each pulse in 'mille second (ms)' level and has been shown in Fig. 3b below, where the periodicity of this power pulse is found to be approximately 7 ms.

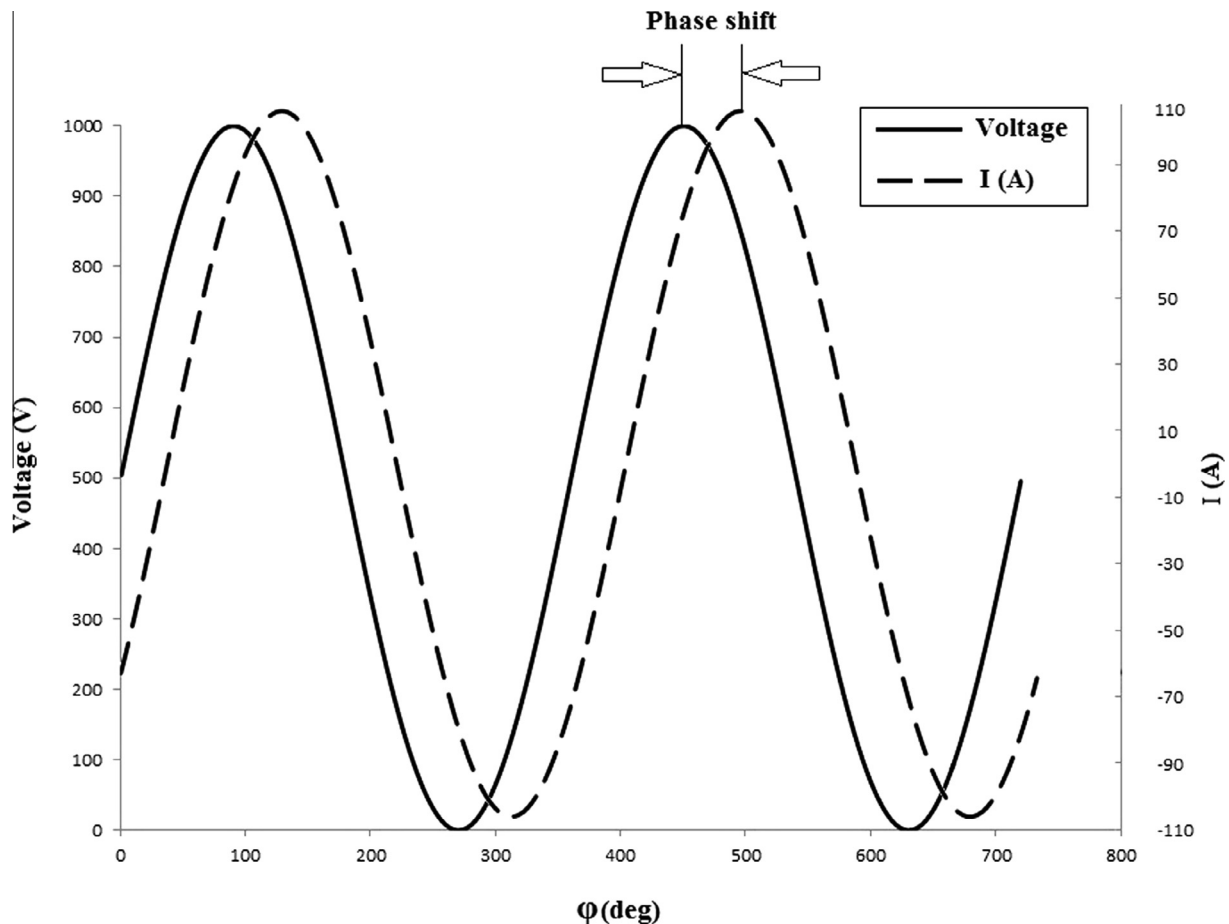


Fig. 3a. Voltage and current waveform for one of the phase with an inductive load.

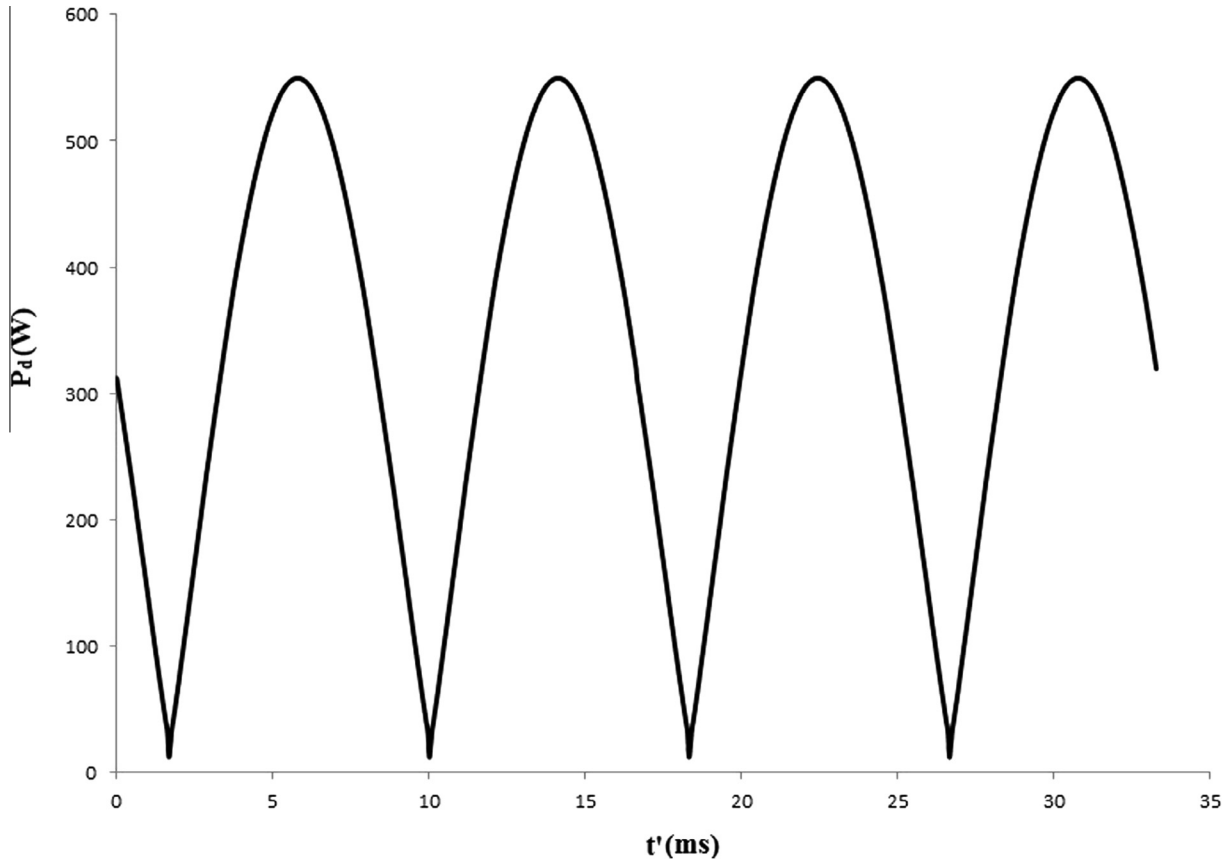


Fig. 3b. Transient power pulse by IGBTs and diodes for all three phases when $P_d = 245$ W.

3.1.1. Averaging of power pulses

In general for a low frequency power pulse, cycle-by-cycle junction temperature fluctuation occurs. As frequency increases, thermal inertia of the junction smooth out instantaneous temperature fluctuations and the junction responds more to average rather than fluctuating power dissipation. Hence, the pulse is averaged (area weighted) over a span of '1 s' considering two types of output current.

- (a) $P_{d,av} = 245$ W ($I = 75$ A as peak value current)
- (b) $P_{d,av} = 347$ W ($I = 75$ A as rms value current)

The above two values of average power dissipation have been considered for rest of the study.

3.2. Heat sink modelling

To dissipate this huge amount of heat from the IGBT assembly by means of conduction and radiation, a heat sink is designed very judiciously and is attached to the base plate of this assembly. Referring to datasheet of the above IGBT module, it has been estimated that the net area of the heat sinking baseplate for the entire assembly is approximately $186 \text{ mm} \times 108 \text{ mm}$. Therefore, to dissipate the above amount of heat, a copper heat sink of dimension $400 \text{ mm} \times 400 \text{ mm} \times 170 \text{ mm}$ is selected and attached to the inverter assembly to make further study on this. Black anodized aluminium ($\varepsilon = 0.9$) has been considered as surface coating of the above heat sink.

4. Governing equations

The Melcosim simulation tool is a well validated product in corporate R&D for power electronics simulation which can be seen in

reference of Wong [9] and it offers a relatively exact and fast method for loss calculation of IGBTs and diodes. The model data for the IGBT modules are based on their respective data sheet values. The calculation of conduction and switching losses of IGBTs and free-wheeling diodes are done based on the application parameters like e.g. DC link voltage, output frequency, switching frequency, modulation index and the power factor ' $\cos \varphi$ '. The corresponding PWM duty is simply calculated by comparing the count value of an up down counter of micro controller with a reference voltage which is sinusoidal in this case.

The power loss is calculated by the following analytical equation taking into account the interval mean values of saturation voltages and current being integrated over entire cycle. By consideration of duty cycle in that equation the mean power of each device can be calculated as follows.

$$P_{CD}(IGBT) = \sum_{\text{phase}=0}^{2\pi} I_C \times V_{CE(sat)} \times \text{Duty(on)} \quad (1)$$

$$P_{CD}(FWDi) = \sum_{\text{phase}=0}^{2\pi} I_C \times V_{CE(sat)} \times \text{Duty(off)} \quad (2)$$

$$P_{SW}(IGBT) = \sum_{\text{phase}=0}^{2\pi} E_{ON} + E_{OFF} \quad (3)$$

$$P_{SW}(FWDi) = \sum_{\text{phase}=0}^{2\pi} E_{rr} \quad (4)$$

To account for the thermal radiation occurring from heat sink surfaces, a Scilab code is written to estimate the thermal resistance (i.e. combined effect of surface resistance and space resistance)

offered between two parallel infinite plates. Referring to M.F. Modest [10], the above sentence can be well conceptualized with the help of the Fig. 4a.

The amount of radiation heat transfer exchanged between the two surfaces maintained at T_1 and T_2 are written as

$$Q_1 = \frac{\sigma(T_1^4 - T_2^4)}{\frac{1-\epsilon_1}{A_1\epsilon_1} + \frac{1}{A_1F_{12}} + \frac{1-\epsilon_2}{A_2\epsilon_2}} = -Q_2 \quad (5)$$

In the Fig. 4b, a typical channel is shown formed by two adjacent fins of a plate-fin heat sink. The Eq. (5) needs modification for a finite geometry of the parallel plates, which has been discussed in the article of Younes Shabany [11].

Considering the channel surface of finite size to be diffuse and gray, and the surrounding medium comparatively large enough, the net radiation heat transfer rate from this channel can be expressed as

$$Q_{ch} = \frac{\sigma(S + 2H)L(T_c^4 - T_a^4)}{\frac{1-\epsilon}{\epsilon} + \frac{1}{F_{sa}}} \quad (6)$$

where F_{sa} represents channel view factor which is the total view factor between walls and the base of channel and its surrounding. As copper heat sink is used here in this study, therefore the thermal resistance from case to sink (R_{cs}) has been taken as zero to avoid further complexities in the study.

Assuming the heat sink temperature to be T_c , the total radiation heat transfer rate from heat sink is expressed as

$$Q_{total} = (n-1)Q_{ch} + [nt(L + 2H) + 2HL + 2t_b(L + W)]\sigma\epsilon(T_c^4 - T_a^4) \quad (7)$$

Following the above expression, the equivalent radiation heat transfer coefficient (h_r) can be calculated as;

$$h_r = \frac{Q_{total}}{A_{hs}(T_c - T_a)} \quad (8)$$

A more accurate estimation for actual radiation heat transfer rate (i.e. where temperature along the fins are not isothermal) can be made by considering the fin equation to account and is expressed as

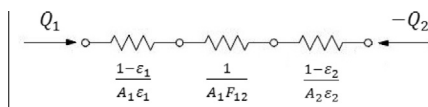
$$Q_{hs,r} = \eta_{hs}A_{hs}h_r(T_c - T_a) \quad (9)$$

The transient temperature equation to evaluate junction temperature response over time (please refer B.W. Williams [12]) for the IGBT module considering conduction and radiation occurring at heat sink surfaces can be written as

$$P_d = -k\frac{A}{l} + \rho A l C_p \frac{\partial T_c}{\partial t} + Q_{hs,r} \quad (10)$$

Once the T_c values are obtained from Eq. (10) at each time step, with the help of Eq. (11) T_j values are calculated at each time step level.

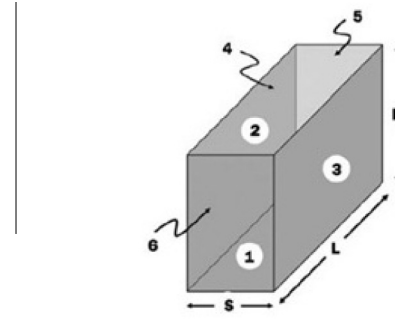
$$T_j = T_c + R_{jc} \times P_d \quad (11)$$



Radiative resistances for an infinite parallel plate

(a)

Fig. 4a. Radiative resistances for an infinite parallel plate.



Channel of a heat sink with finite length

(b)

Fig. 4b. Channel of a heat sink with finite length.

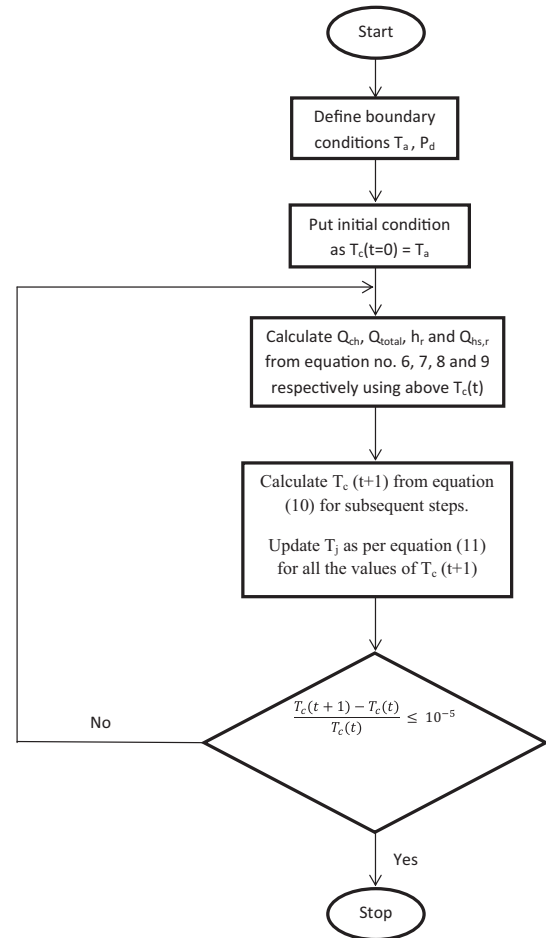


Fig. 5. Flowchart showing the detail of numerical steps considered in the study.

5. Numerical technique and results

In most of the literatures, Eq. (10) is solved either by Cauer or Foster RC network model. In both models the thermal resistance of IGBT cold plate and heat sink materials are calculated by means of RC network where product of R and C is presumed to be a function of material properties. This network interpretation

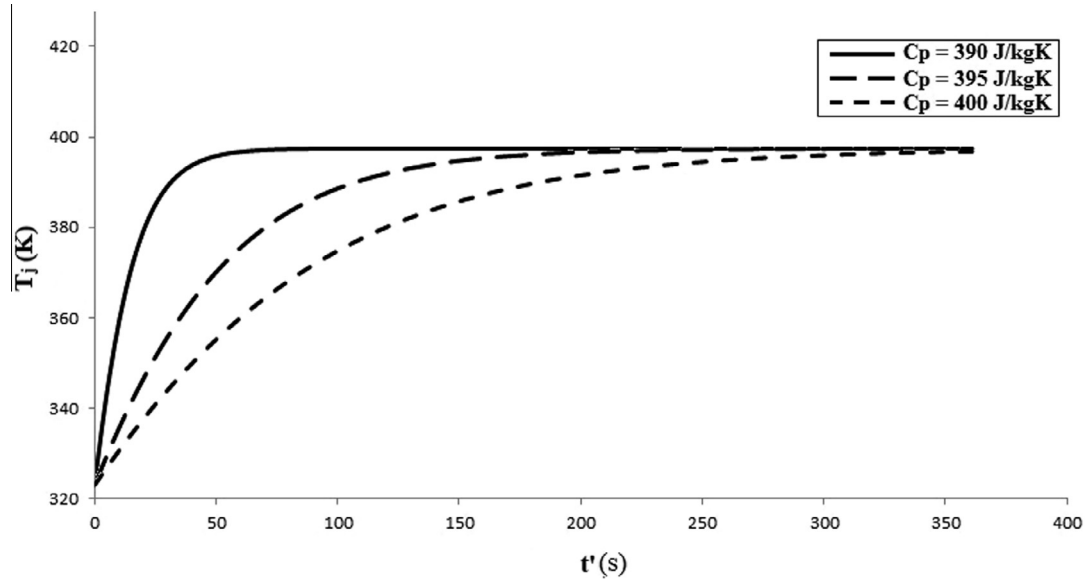


Fig. 6. Variation in steady state reaching time (t') with change in the value of C_p .

method to calculate thermal resistance values holds good for smaller geometries however for bigger geometries the method has shown a lot of discrepancies. Especially for large heat sink, the thermal radiation becomes active with increasing surface area which can seldom be addressed by limited scope of RC network model. Therefore, to overcome this situation, a Scilab code has been written to describe the importance of thermal radiation coming from heat sink in increasing the operating range of entire IGBT module.

The Eqs. ((6)–(11)) have been solved iteratively to find out the values of T_j at every time step (t') level. The above flowchart

(i.e. Fig. 5) explains the steps followed in solving the set of equation systematically. A finite difference discretization of the transient Eq. (10) is done to calculate T_c at each forward time steps until the system reaches a complete steady state. The initial condition considered for the above case is $T_c(t' = 0) = T_a$, based on which the temperature for the remaining time steps have been evaluated. The numerical time step has been taken here as '1 s' and almost 800 iterations are performed for the case temperature to reach steady state. Crucial heat sink parameters have been changed to investigate their effect on change in junction temperature and time taken for the junction temperature to reach steady state.

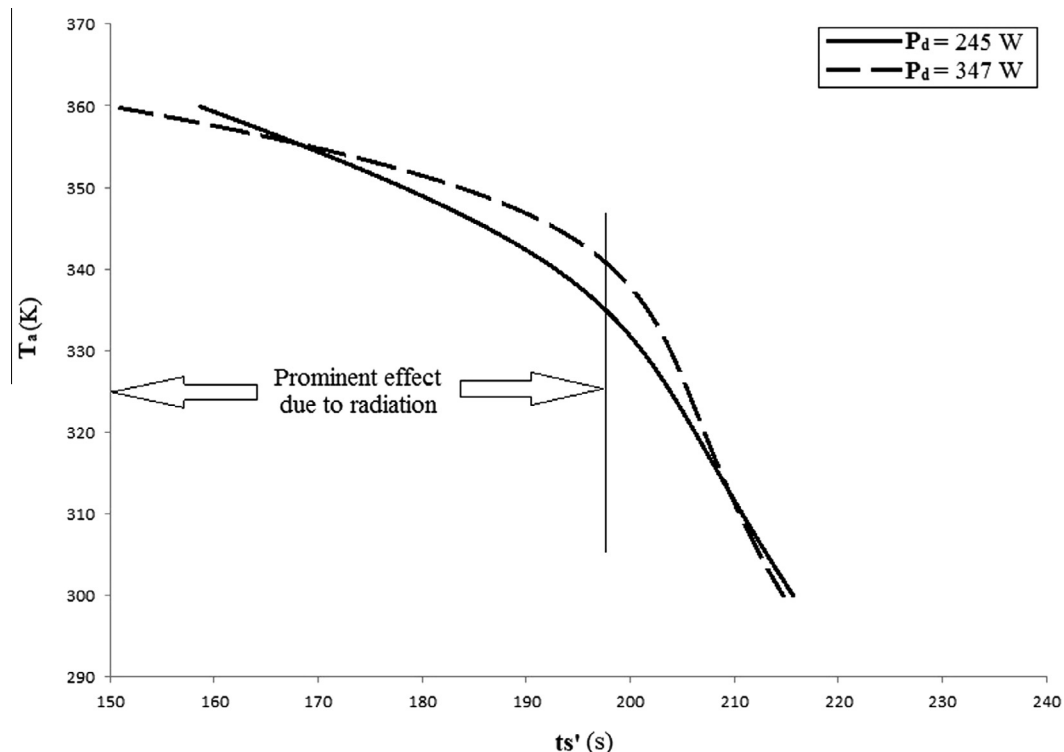


Fig. 7. Variation in reaching the steady state time with increasing ambient temperature (T_a).

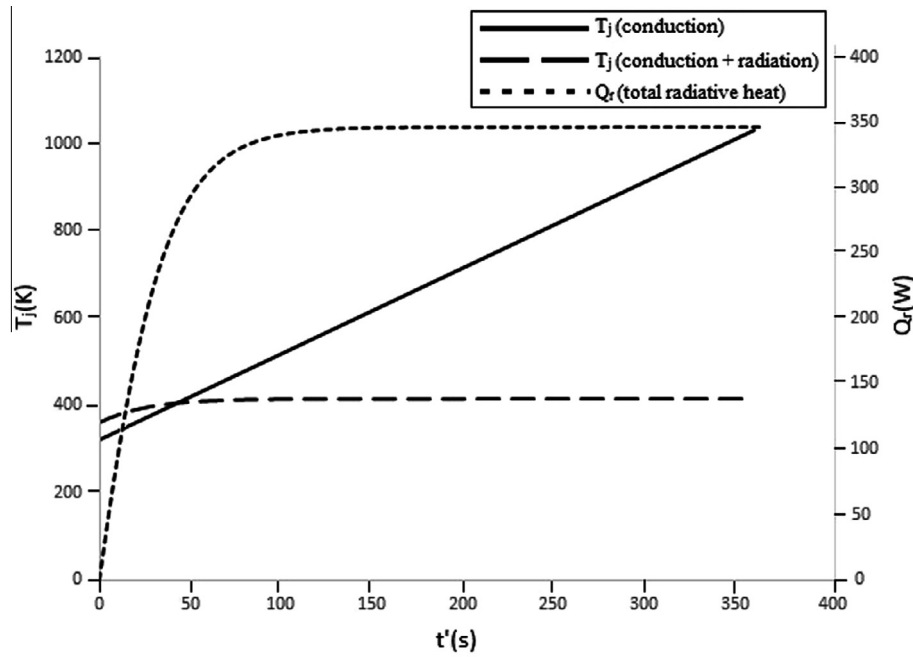


Fig. 8. Comparison of junction temperature (T_j) with and without radiation when $P_d = 347$ W.

With the above input conditions, the first hand results have been obtained for $P_d = 347$ W and $T_a = 320$ K which is presented below with discussions. The Fig. 6 shows that the time to reach the steady state is merely varying between 100 s and 350 s depending on the variation of specific heat capacity of the heat sink material. To emphasis important effects of heat sink parameters on t' , the value of reaching steady state time (ts') is fixed at 100 s and therefore the specific heat is chosen as 390 J/kg K for the entire study made.

To understand the pronounced effect of radiation in reaching steady state faster at higher ambient temperatures, a series of simulations are carried out with increasing ambient conditions applied and are depicted in Fig. 7. The figure clearly demonstrates that when the value of T_a is raised from 300 K to 340 K, rate of reduction in time to reach the steady state is much lower than compared to when T_a raised beyond 340 K. It can be also seen from the figure that difference between time gradients at two ambient temperature

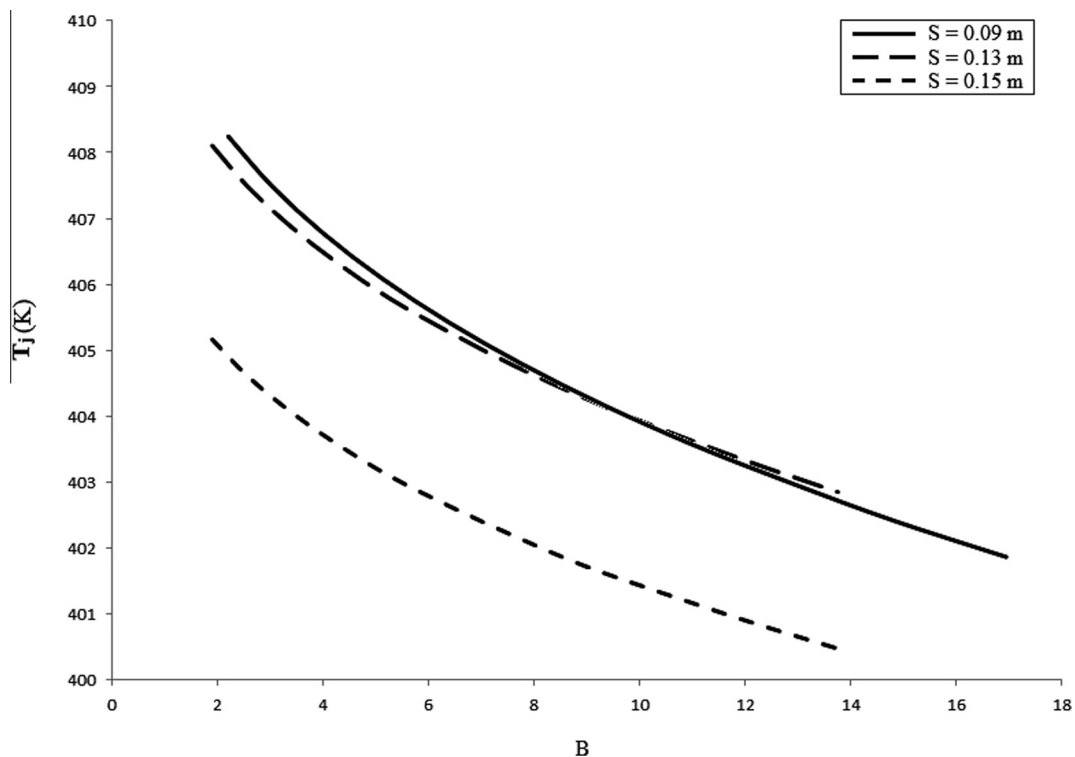


Fig. 9. Change in junction temperature (T_j) with increasing 'B' at different values of 'S'.

Table 1Values of junction temperature (T_j) with increasing 'B' at different values of 'S' while $P_d = 245$ W and $T_a = 360$ K.

$S = 0.03$		$S = 0.05$		$S = 0.07$		$S = 0.09$		$S = 0.11$		$S = 0.13$		$S = 0.15$		$S = 0.17$	
B	T_j	B	T_j	B	T_j	B	T_j	B	T_j	B	T_j	B	T_j	B	T_j
4.24	406.09	3.19	405.62	2.53	407.60	2.21	408.25	2.22	404.17	1.90	408.11	1.90	405.17	1.90	402.63
6.03	404.67	4.49	404.58	3.51	406.73	3.04	407.49	3.04	403.52	2.58	407.48	2.58	404.60	2.58	402.12
7.41	406.01	6.03	403.60	4.67	405.91	4.01	406.77	4.00	402.90	3.37	406.89	3.37	404.08	3.37	401.64
9.64	404.73	6.90	406.54	5.99	405.12	5.13	406.09	5.11	402.32	4.27	406.33	4.27	403.58	4.27	401.19
10.98	406.48	8.65	405.61	7.50	404.37	6.38	405.43	5.28	408.95	5.26	405.79	5.26	403.10	5.26	400.76
13.51	405.30	10.58	404.72	9.17	403.64	7.78	404.79	6.39	408.35	6.41	405.27	6.41	402.63	5.05	410.38
16.30	404.18	12.79	403.87	11.06	402.94	9.32	404.17	7.64	407.78	7.64	404.76	7.64	402.18	6.01	409.91
17.27	406.42	15.19	403.05	11.01	407.77	11.01	403.57	8.99	407.22	8.99	404.27	8.96	401.73	7.04	409.45
20.16	405.38	15.29	406.74	12.87	407.07	12.87	402.99	10.48	406.67	10.48	403.79	10.48	401.31	8.15	409.00
23.33	404.38	17.61	405.92	14.81	406.39	14.81	402.42	12.07	406.13	12.07	403.31	12.07	400.89	9.33	408.56
26.79	403.42	20.27	405.16	16.95	405.74	16.95	401.87	13.76	405.61	13.76	402.85	13.76	400.48	10.64	408.13

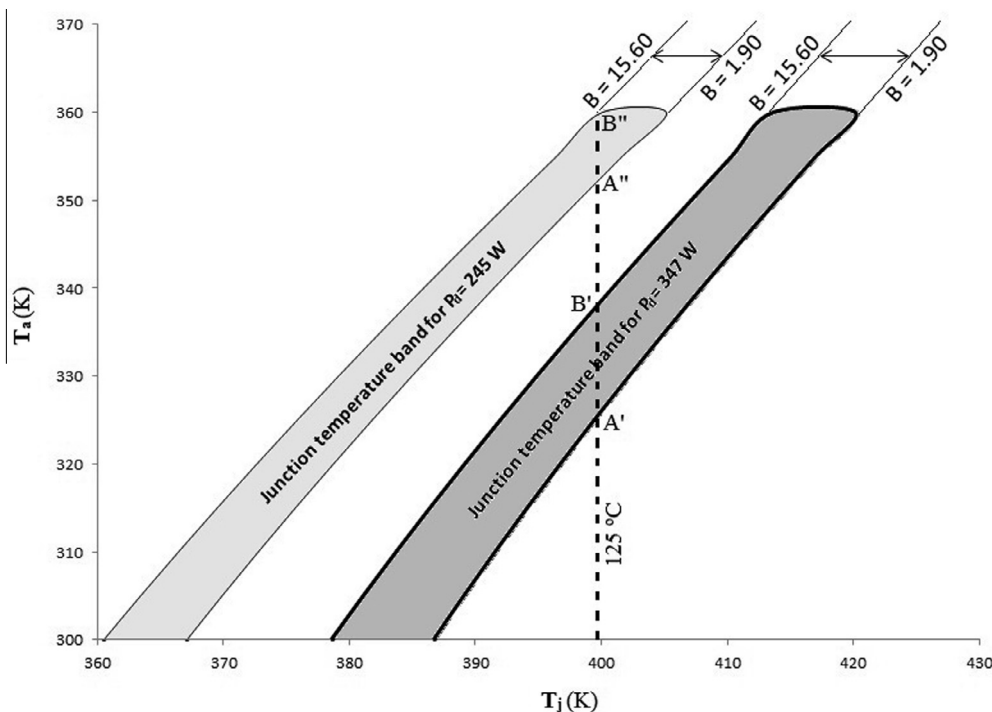
ranges becomes more as the power dissipation from IGBT shoots up from 245 W to 347 W.

The contribution of thermal radiation in maintaining the junction temperature at $T_j = 400$ K can be better assessed from the above Fig. 8. In the figure, it can be clearly seen that the junction temperature is increasing continuously with time if the system is cooled by conduction alone, whereas with considering radiation occurring from the heat sink surfaces the system reaches a steady value of $T_j = 400$ K at a time $t' = 150$ s. The total radiative heat dissipated by the heat sink for the above case is close to 350 W, which is a significant amount and hence thermal radiation acts as a major driver to remove heat faster from these type of systems.

The study is further extended to see significant effects of thermal radiation in bringing the steady state faster by changing crucial heat sink parameters. Apart from other parameters, it is noted that there are three important heat sink parameters on which time to reach the steady state mainly depends and they are (i) gap between two fins (S), (ii) fin thickness (t) and (iii) base thickness (t_b). To present the important observations systematically here in this study, a parameter named B is introduced which

shows the ratio of fin thickness (t) to base thickness (t_b) at a random value of S. Keeping $P_d = 245$ W and $T_a = 360$ K fixed, a lot of simulations have been performed to calculate the IGBT junction temperatures at various values of B for a particular value of S and the results are recorded. It has been thus found that with the existing set up of IGBT and heat sink, junction temperature drops with an increasing B for $S = 0.09$ m, 0.13 m and 0.15 m as can be seen in Fig. 9. Further increasing the value of B for other values of S leads to increase in junction temperature very rapidly and hence are not of much use for this study however to get a quantitative idea of the entire investigation please refer to Table 1. Inside the figure it can be seen that junction temperature curve for $S = 0.09$ and 0.13 are almost alike whereas for $S = 0.15$ m, the magnitude of curve falls significantly which means that as no. of fins reduce it increases the radiation heat transfer from heat sink surface. For the above case, no. of fins calculated to be four where the junction temperature is found least i.e. 400.48 K.

Likewise, to have a better insight of above description, the junction temperature bands for $P_d = 245$ W and $P_d = 347$ W are plotted for an effective range of B against the increasing ambient temperature (T_a) in Fig. 10. Inside the figure it can be observed that

**Fig. 10.** Junction temperature (T_j) bands with increase in ambient temperature for a range of B.

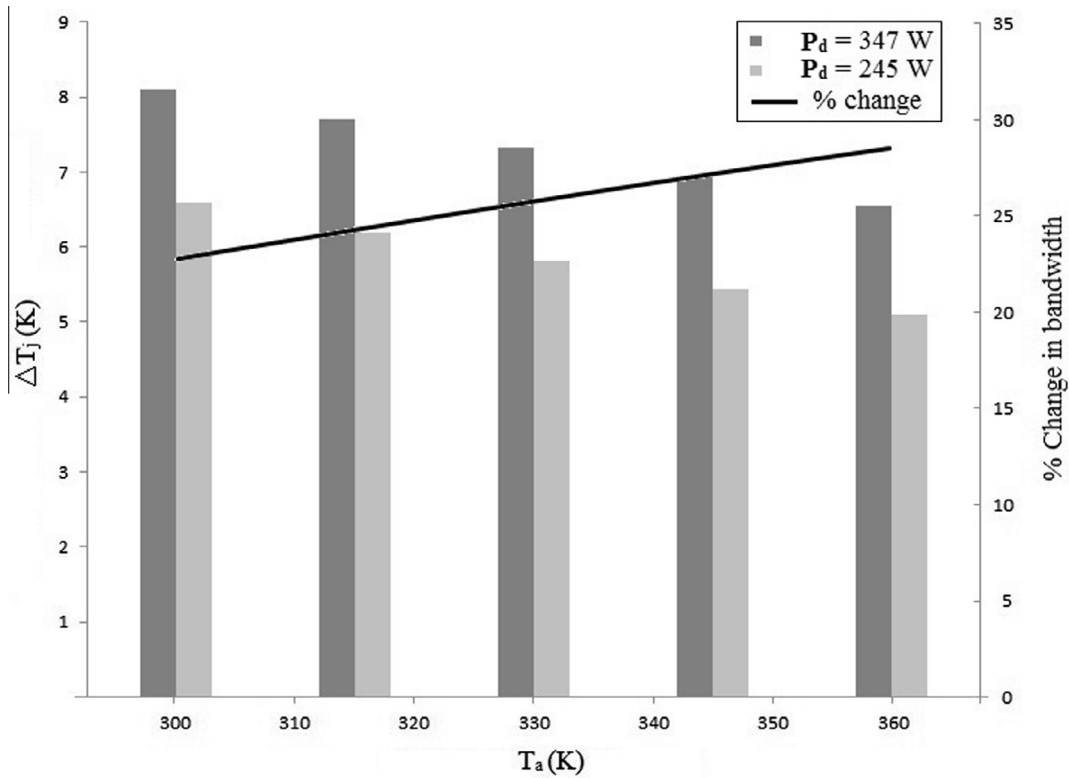


Fig. 11. % change in junction temperature bandwidth with an increasing value of T_a .

Table 2

The difference in junction temperature bandwidth between $P_d = 347$ W and $P_d = 245$ W with an increasing ambient temperature level.

T_a	$P_d = 347$ W			$P_d = 245$ W			% diff
	$T_j(B = 1.904)$	$T_j(B = 15.609)$	ΔT_j	$T_j(B = 1.904)$	$T_j(B = 15.609)$	ΔT_j	
300.00	386.75	378.65	8.10	367.09	360.50	6.59	22.86
305.00	389.16	381.19	7.97	369.89	363.43	6.46	23.36
310.00	391.65	383.80	7.84	372.77	366.43	6.33	23.87
315.00	394.20	386.49	7.71	375.71	369.51	6.20	24.37
320.00	396.83	389.25	7.58	378.72	372.65	6.07	24.86
325.00	399.53	392.08	7.45	381.81	375.87	5.94	25.35
330.00	402.29	394.97	7.32	384.96	379.14	5.82	25.84
335.00	405.13	397.94	7.19	388.17	382.48	5.69	26.32
340.00	408.03	400.97	7.06	391.45	385.89	5.57	26.79
345.00	411.00	404.07	6.93	394.79	389.35	5.44	27.26
350.00	414.03	407.23	6.80	398.19	392.87	5.32	27.72
355.00	417.12	410.45	6.67	401.65	396.44	5.21	28.16
360.00	420.28	413.73	6.55	405.17	400.07	5.09	28.60

the slope for band $P_d = 245$ W is less than compared to band $P_d = 347$ W which means that the increment in junction temperature is less for band $P_d = 347$ W compared to band $P_d = 245$ W for the same ambient temperature rise. This is because of the intense effect of thermal radiation by heat sink at higher power dissipation of IGBT. Moreover it can be noticed that the band width (i.e. from $B = 1.90$ to 15.60) of $P_d = 347$ W is more than band width of $P_d = 245$ W at any value of ambient temperature considered which means that at higher power dissipation rates the reduction in junction temperature is more compared to lower dissipation rates for same range of B . Focussing onto other side of the figure, it is seen that maximum junction temperature line (i.e. $T_{j,max} = 125^\circ\text{C}$) intersects the junction temperature bands of $P_d = 347$ W and $P_d = 245$ W at A'B' and A''B'' respectively. Points A'B' implies that when the IGBT module dissipates a power of $P_d = 347$ W, allowances for the ambient temperature increases with increases in value of B . The ambient temperature (T_a)

corresponding to point B' is much higher than that of point A'. Hence this line indirectly gives a complete guidance about the value of B we should maintain at a particular ambient temperature to remain within maximum junction temperature limit.

Fig. 11 gives a fairly better idea about the % change in junction temperature bandwidth regarding the above discussion and a detail quantification of data is listed in below Table 2. The figure clearly demonstrates that % change in junction temperature reduction between two bands (i.e. $P_d = 347$ W and $P_d = 245$ W) goes up with the increase in ambient temperature level. This is due to the fact that for same power dissipation of IGBT, thermal radiation from heat sink increases with an increasing ambient temperature level.

6. Conclusion

The above study summarizes that the IGBT and diode assemblies present inside a three phase inverter dissipate heat at a very high

frequency pulse for which the junction temperature rises with time. Thermal radiation occurring from plate fin heat sink attached to the unit brings a faster steady state condition to the transient growth of junction temperature. The study also highlighted permissible limits of the ambient temperature for a particular value of B to remain within the maximum allowable junction temperature. Increasing ambient temperature enhances thermal radiation from heat sink surfaces and thereby helps the junction temperature to become steady at a much faster rate for same amount of power dissipated by the IGBT and diode assembly. Small change in the value of specific heat (C_p) of heat sink material has fairly big impact in increasing the steady state reaching time.

References

- [1] T. Kojima, Y. Yamada, M. Ciappa, M. Chiavarini, W. Fichtner, A novel electro-thermal simulation approach to power IGBT module for automotive traction applications, *R&D Review of Toyota CRDL* 39 (2004) 27–32.
- [2] J. Popovic, M. Milanovic, D. Dolinar, B. Klopčič, Thermal analysis of the half-bridge IGBT power module with analytical, numerical and experimental methods, *Przeglad Electrotechniczny (Electrical Review)* 87 (2011) 145–148.
- [3] Ke Ma, F. Blaabjerg, M. Liserre, Electro-thermal Model of Power Semiconductors Dedicated for Both Case and Junction Temperature Estimation, Department of Energy Technology, Aalborg University, Denmark.
- [4] R. Schnell, Simulation tool for IGBT modules, ABB Switzerland Ltd.
- [5] M. Angira, K. Rangra, A novel design for low insertion loss, multi-band RF-MEMS switch with low pull-in voltage, *Eng. Sci. Technol. Int. J. (Elsevier)* 19 (2016) 171–177.
- [6] A. Pal, A. Sarkar, Analytical study of dual material surrounding Gate MOSFET to suppress short-channel effects (SCEs), *Eng. Sci. Technol. Int. J. (Elsevier)* 17 (2014) 205–212.
- [7] M.H. Moaiyeri, M. Nasiri, N. Khastoo, An efficient ternary serial adder based on carbon nanotube FETs, *Eng. Sci. Technol. Int. J. (Elsevier)* 19 (2016) 271–278.
- [8] M. Turkyilmazoglu, Performance of direct absorption solar collector with nanofluid mixture, *Energy Convers. Manage. (Elsevier)* 114 (2016) 1–10.
- [9] A. Wong, Switching regulator LED lighting applications, *Automotive Electronics Part II, Power Systems Design (Europe)* (2008) 52–57.
- [10] M.F. Modest, *Radiative Heat Transfer*, Chapter-5, McGraw-Hill, 1993.
- [11] Y. Shabany, Simplified correlations for radiation heat transfer rate in plate-fin heat sinks, *Electron. Cooling Mag.* 08 (2008).
- [12] B.W. Williams, *Principles and Elements of Power Electronics*, Chapter-5, 2006.